Available online at www.sciencedirect.com
ScienceDirect
Ceramics International 37 (2011) 3637–3642
CERAMICS INTERNATIONAL
www.elsevier.com/locate/ceramint

Effect of silicon and heat-treatment temperature on the morphology and mechanical properties of silicon - substituted hydroxyapatite

L.T. Bang [a], K. Ishikawa [b], R. Othman [a,*]

[a] School of Materials and Mineral Resources Engineering, Engineering Campus, Universiti Sains Malaysia, 14300 Nibong Tebal, Penang, Malaysia
[b] Department of Biomaterials, Faculty of Dental Sciences, Kyushu University, Japan

Received 18 April 2011; received in revised form 1 June 2011; accepted 13 June 2011
Available online 6 July 2011

Abstract

The precipitation method was used to synthesize silicon-substituted hydroxyapatite with different Si contents of 0.4, 0.8 and 1.6 wt.% (0.4, 0.8 and 1.6Si-HA) using silicon acetate [$Si(OCOCH_3)_4$] as a Si source. As-synthesized hydroxyapatite (HA) and Si-HA powders/bulks were heat-treated at different temperatures of 1150, 1200 and 1250 °C for 1 h. Pure 0.4Si-HA and 1.6Si-HA were obtained after heat-treatment at all temperatures, whilst α-TCP phase was formed in the 0.8Si-HA sample after heat-treatment at 1250 °C. SEM observation clearly showed that the substitution of Si in HA inhibited the grain growth of Si-HA even at high heat-treatment temperatures (1200 or 1250 °C). The highest diametral tensile strength (DTS) of 15.93 MPa was obtained in the 1.6Si-HA sample after heat-treatment at 1250 °C.

Keywords: C. Mechanical properties; Silicon-substituted hydroxyapatite; Biomaterials; Morphology

1. Introduction

Hydroxyapatite (HA), $Ca_{10}(PO_4)_6(OH)_2$ has been used as a biomaterial in bone grafting, bone tissue engineering and drug delivery system due to its excellent biocompatibility and ability to form a direct chemical bond with hard tissues [1,2]. However, HA shows a low bioactive property due to its low resorbability [3]. The bioactive behaviour of HA has been improved by substituting certain ions in the apatite structure [3–5]. There are various substitutions that exist in the actual human bone mineral, and these include Na, Mg, K, Sr, Zn, Ba, Cu, Al, Fe, F, Cl and Si [6]. Numerous research works [5,7–9] indicated that the addition of Si in HA led to an improvement of the bioactivity and enhancement of bone growth. Besides, Si substituted HA is also able to continuously supply ions which are essential for the process of bone reconstruction and biological processes [10,11].

Si-substituted HA (Si-HA) has been synthesized using different methods such as precipitation and mechano-chemical methods, different Si sources and different Si contents (0–2 wt.%) [4,9,12]. A research work [12] reported that with Si content substitution higher than 2 wt.%, the original structures of HA was destabilized and secondary phases such as α-TCP and calcium phosphate silicate were formed after heat-treatment at 1100 °C or higher. The mechanisms of Si-HA formation and the effect of Si on biological properties of Si-HA has been studied in many research works [6–8,12–20]. However, the heat-treatment behaviour and the effect of Si content on the mechanical properties of Si-HA has hardly been explored.

The aim of this research is to investigate the effect of Si content and heat-treatment temperature on the grain size and mechanical properties of Si-HA. The effect of Si substitution on the different functional groups, such as hydroxyl (OH^-), phosphate (PO_4^{3-}) and silicate (SiO_4^{4-}) groups of Si-HA was also investigated.

2. Experimental procedure

A pure HA powder was prepared by adding slowly 300 ml of 1 M H_3PO_4 (15M, MERCK, 100573, Germany) into a 500 ml solution of 1 M $Ca(OH)_2$ (96% purity, FLUKA, 21181). The amount of reagents was calculated in order to obtain a Ca/P molar ratio which is equal to the stoichiometric HA value of

* Corresponding author. Tel.: +60 124530412; fax: +60 45941011.
E-mail address: radzali@eng.usm.my (R. Othman).

0272-8842/$36.00
doi:10.1016/j.ceramint.2011.06.023

Table 1
Quantities of reagents used and the measured wt.% of Si of the samples.

Sample	Si (wt.%)	$Ca(OH)_2$ (mole)	$Si(OCOCH_3)_4$ (mole)	H_3PO_4 (mole)
0.4Si-HA	0.4	0.5	0.0072	0.2928
0.8Si-HA	0.8	0.5	0.0143	0.2857
1.6Si-HA	1.6	0.5	0.0284	0.2716

10/6. In order to synthesize Si-substituted HA (Si-HA), 500 ml of 1 M H_3PO_4 solution was dripped into a homogeneous solution of 1 M $Ca(OH)_2$ and $Si(OCOCH_3)_4$ (98% purity, SIGMA-ALDRICH) based on the chemical formula $Ca_{10}(PO_4)_{6-x}(SiO_4)_x(OH)_{2-x}$ proposed by Gibson et al. [14]. The amount of reagents were calculated by assuming that one silicate ion would substitute for one phosphate ion based on a stoichiometric HA, Ca/(P + Si) molar ratio = 10/6.

The Si-HA powder was synthesized with three different compositions of 0.4, 0.8 and 1.6 wt.% Si (0.4, 0.8 and 1.6Si-HA) (Table 1). The synthesis of HA and Si-HA powders were carried out in a water bath at 40 °C where vigorous stirring was simultaneously applied with a rotation speed of 400 rpm. The pH of the solution was controlled at around 9 by the addition of an ammonia solution 29% (J.T. Baker, USA).

The resulting precipitates were aged in the mother solution for 24 h at room temperature. The aged precipitates were filtered, washed 3 times with distilled water in order to remove any other residues before being dried in an oven at 90 °C for 12 h. The resultant powders were then hydraulically pressed in a die with 13 mm diameter at 50 MPa. The compacts and the as-synthesized powders were heat-treated using a Lenton 1500 furnace at 1150, 1200 and 1250 °C in air for 1 h.

The as-synthesized and heat-treated powders were characterized using an X-ray diffractometer (XRD), D5000 Siemens. The lattice parameters (a and c) of HA and Si-HA samples were calculated at the (0 0 2) and (3 0 0) Miller planes family from the XRD patterns. Fourier transform infrared (FTIR) spectroscopy was used to study the effect of Si substitution on the different functional groups, such as OH^-, PO_4^{3-} and SiO_4^{4-} of HA and Si-HA using a Perkin-Elmer FT-IR 2000, FTIR spectrometer. The morphology of the heat-treated samples were investigated using a field emission scanning electron microscope (FESEM), LEO Supra 55 VP.

The densities of the heat-treated HA and Si-HA samples were measured using the Archimedes' principle. The diametral tensile strengths (DTS) of the heat-treated compacts were tested at a strain rate of 0.5 mm/min. In this test, a disk sample was placed between two platens and then vertically compressed until it broke [21]. During loading, the applied force was recorded and the tensile stress is calculated using Eq. (1):

$$\mathrm{Ft} = \frac{2P_{\max}}{\pi h d} \quad (1)$$

where P_{max} is maximum load at failure (N), h is the thickness of the compact (mm), d is diameter of compact (mm) [22]. Five samples per batch were used for the lattice parameter measurements, density and DTS tests. Errors of approximately ±2 and 0.05% were observed in the density/DTS test, and lattice parameter measurements, respectively.

3. Results and discussion

3.1. XRD analysis

Fig. 1 shows the XRD patterns of the as-synthesized HA and Si-HA powders. The XRD peaks of Si-HA show increasing broadening and decreasing intensity with increasing Si content (Fig. 1(b)–(d)). This is attributed to a loss of crystallinity by the isomorphous substitution of PO_4^{3-} by SiO_4^{4-} during synthesis [16].

After heat treatment at 1150 to 1250 °C, pure HA, 0.4Si-HA and 1.6Si-HA were formed, no secondary phases are detected (Fig. 2(a), (b) and (d)). However, a new phase, α-TCP, is clearly observed in the 0.8Si-HA sample heat-treated at 1250 °C (Fig. 2(c)). This indicates that the decomposition of Si-HA had occurred. The decomposition of Si-HA into α-TCP was also observed in other research works [4,10,13,17]. In Fig. 2, only the XRD patterns of HA and Si-HA samples heat-treated at 1250 °C are shown.

The lattice parameters of the heat-treated HA and Si-HA samples at different temperatures are listed in Table 2. It can be seen that the lattice parameters of Si-HA are relatively larger than that of pure HA. This can be explained by the substitution of PO_4^{3-} by SiO_4^{4-} which contributed to the increase in the lattice parameters of Si-HA [10,16,18]. As a result, the increase in the lattice parameters of Si-HA resulted in a slight shift of the Si-HA peaks to a lower Bragg's angle compared to pure HA, as shown in Fig. 3.

3.2. FTIR analysis

Fig. 4 shows the FTIR spectra of the as-synthesized HA and Si-HA samples where a similar pattern was observed for all these samples. All of the spectra show a weak band at around 630 cm^{-1} corresponding to the OH^- group [13,14]. The spectra of as-synthesized HA/Si-HA also show the vibrational mode present for PO_4^{3-} group at about 920 cm^{-1}

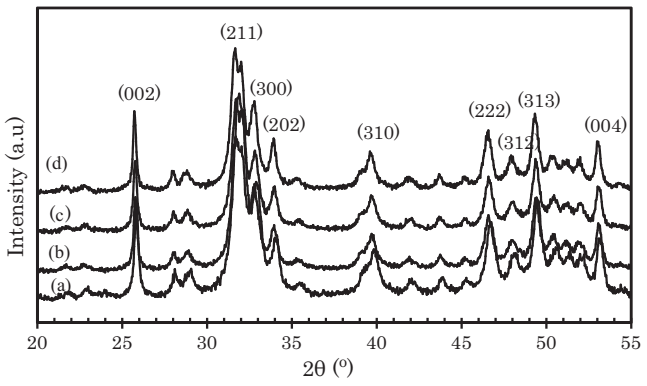

Fig. 1. XRD patterns of the as-synthesized HA and Si-HA powders: (a) pure HA, (b) 0.4Si-HA, (c) 0.8Si-HA and (d) 1.6Si-HA.

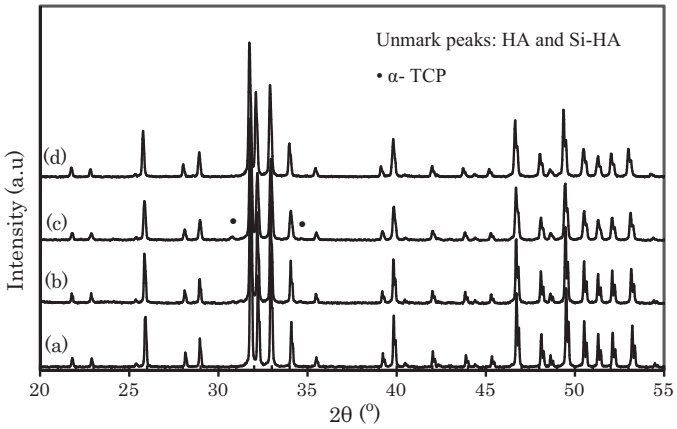

Fig. 2. XRD patterns of HA and Si-HA powders after heat-treatment at 1250 °C: (a) pure HA, (b) 0.4Si-HA, (c) 0.8Si-HA and (d) 1.6Si-HA.

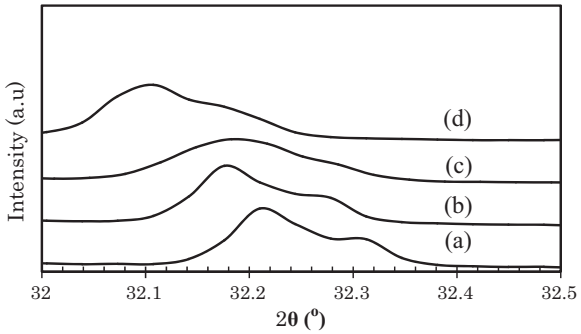

Fig. 3. Peak shift for Si-HA samples with increasing silicon content after heat-treatment at 1250 °C: (a) pure HA, (b) 0.4Si-HA, (c) 0.8Si-HA and (d) 1.6Si-HA.

(υ_1), 1092–1101 cm^{-1} (υ_2), 1027–1039 cm^{-1} (υ_3) and 603–566 cm^{-1} (υ_4) [10,14,19,23].

In Fig. 4(b)–(d), with increasing Si content, the band intensity corresponding to P–O (most noticeably at about 962–963 cm^{-1}) and the OH^- group at about 630 cm^{-1} decreases. In particular, the appearance of the bands at 801.09 cm^{-1} and 505.20 cm^{-1}, 893.15 cm^{-1} and 503.01 cm^{-1}, and 891.85 cm^{-1} and 758.38 cm^{-1} in the 0.4, 0.8 and 1.6Si-HA samples, respectively, are related to SiO_4^{4-} group [10,15,24]. This suggests that phosphate site was substituted by Si in the HA structure [7,19].

The FTIR spectra of the heat-treated powders at different temperatures of 1150, 1200 and 1250 °C are quite similar, where Fig. 5 (at 1250 °C) is taken as the representative spectra. Nonetheless, these spectra show significant difference from the as-synthesized samples. The most notable effect of Si substitution on the FTIR spectrum of HA is the decrease in both the PO_4^{3-} group bands at about 1098, 1042–1047, 962 cm^{-1} and a shoulder at 571–601 cm^{-1}, and the OH^- group bands at 631 cm^{-1} compared to the as-synthesized samples. This behaviour was associated with the incorporation of Si in the HA lattice, i.e. the incorporation of SiO_4^{4-} into the PO_4^{3-} group and the loss of OH^- group in order to compensate for the extra negative charge of the SiO_4^{4-} group [12,17]. Another research work [9] also stated that the negative charge of the SiO_4^{4-} ions substituting PO_4^{3-} is balanced by the creation of hydroxide vacancies, leading to the following chemical formula of Si-HA:

$$Ca_{10}(PO_4)_{6-x}(SiO_4)_x(OH)_{2-x} \qquad \text{with} 0 \le x \le 2 \qquad (2)$$

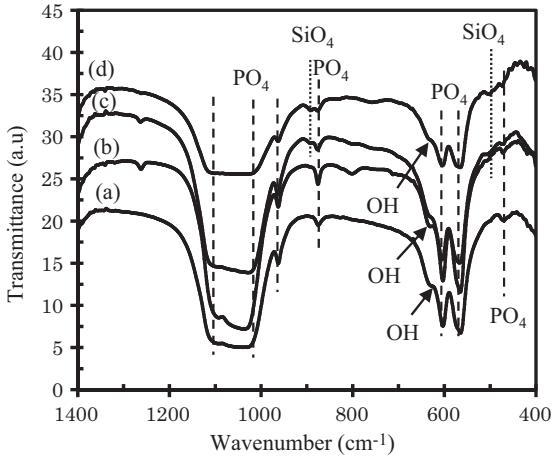

Fig. 4. FTIR spectra of as-synthesized HA and Si-HA powders: (a) pure HA, (b) 0.4Si-HA, (c) 0.8Si-HA and (d) 1.6Si-HA.

3.3. Effect of Si on the grain growth of Si-HA

The effect of Si substitution on the grain size of the heat-treated Si-HA samples at different heat-treatment temperatures was studied using SEM, where only the micrographs at 1200 °C are shown (Fig. 6). The grain size of Si-HA samples is clearly finer than that of pure HA sample and this decreases with increasing Si content. There had been many reports on the effect of Si on the grain size of Si-HA. Palard et al. [25] reported that the grain size of Si-HA decreased markedly when Si content was less than 0.5 wt.% but decreased slightly when higher Si contents were used. Li

Table 2
Lattice parameters of HA and Si-HA samples after heat-treated at different temperatures of 1150, 1200 and 1250 °C.

Sample	Heat-treatment at 1150 °C		Heat-treatment at 1200 °C		Heat-treatment at 1250 °C	
	$a \pm 0.0005$ (Å)	$c \pm 0.0005$ (Å)	$a \pm 0.0005$ (Å)	$c \pm 0.0005$ (Å)	$a \pm 0.0005$ (Å)	$c \pm 0.0005$ (Å)
Pure HA	9.4366	6.8905	9.4366	6.8810	9.4174	6.8732
0.4Si-HA	9.4316	6.8952	9.4127	6.8818	9.4177	6.8907
0.8Si-HA	9.4403	6.9036	9.4191	6.8831	9.4213	6.8956
1.6Si-HA	9.4655	6.9271	9.4168	6.8894	9.4272	6.9096

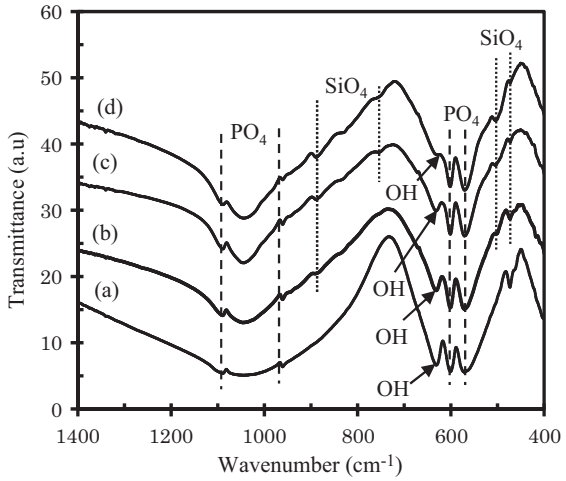

Fig. 5. FTIR spectra of HA and Si-HA powders after heat-treatment at 1250 °C: (a) pure HA, (b) 0.4Si-HA, (c) 0.8Si-HA and (d) 1.6Si-HA.

et al. [26] also reported that the effect of Si on the grain size of Si-HA was also more significant when SiO_4 content used was less than 2 wt.%. They pointed out that the grain size decreased less when Si content reached a certain value due to the formation of secondary phases such as α-TCP [25,26]. In general, these research works [25,26] agreed that the grain size of Si-HA decreases with increasing Si content, and Gibson et al. [13] suggested that a higher value of activation energy (183–205 kJ/mol) was required for the grain growth of Si-HA compared to stoichiometric HA (141 kJ/mol). This indicates that Si effectively impedes the grains from coarsening during the heat-treatment.

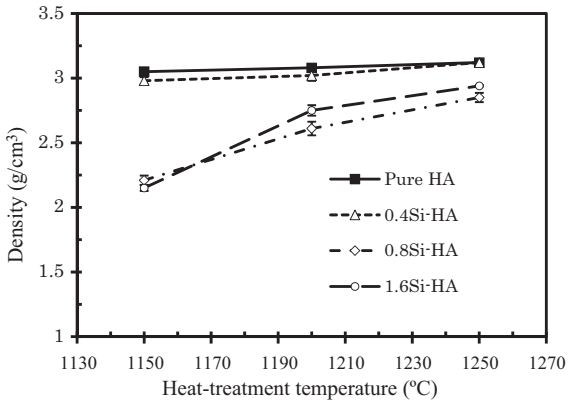

Fig. 7. Density of HA and Si-HA samples heat-treated at 1150, 1200 and 1250 °C.

3.4. Evaluation of mechanical properties

Fig. 7 shows the bulk density of HA and Si-HA samples as a function of the heat-treatment temperatures. The density of pure HA and 0.4Si-HA are similar and slightly increases with increasing heat-treatment temperatures. By comparison, the density of 0.8Si-HA and 1.6Si-HA increases much more with heat-treatment temperature. At the same heat-treatment temperature, the density of Si-HA is lower than that of pure HA and decrease with increasing Si content. This is due to the fact that the unit cell parameters of Si-HA was increased with increasing Si substitution [12,15]. However, at 1200 and 1250 °C, the density of 1.6Si-HA is higher than that of 0.8Si-HA. This is possibly due to the formation of a small amount of α-TCP phase in the 0.8Si-HA. At high temperatures, the effect of Si on the density of Si-HA

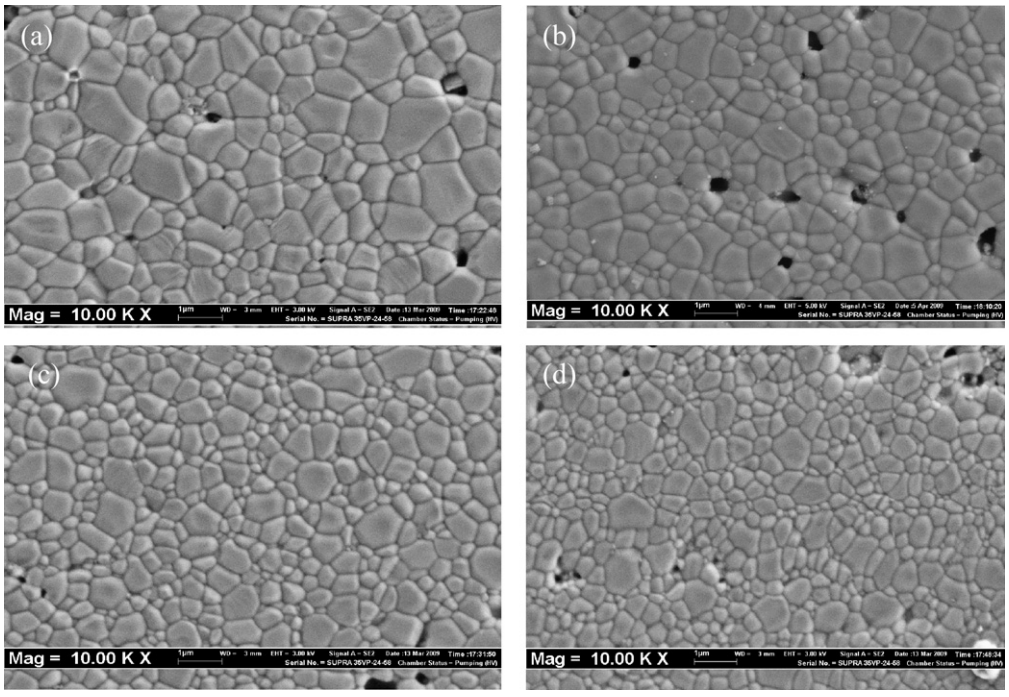

Fig. 6. SEM micrographs of HA and Si-HA compacts heat-treated at 1200 °C: (a) pure HA, (b) 0.4Si-HA, (c) 0.8Si-HA and (d) 1.6Si-HA.

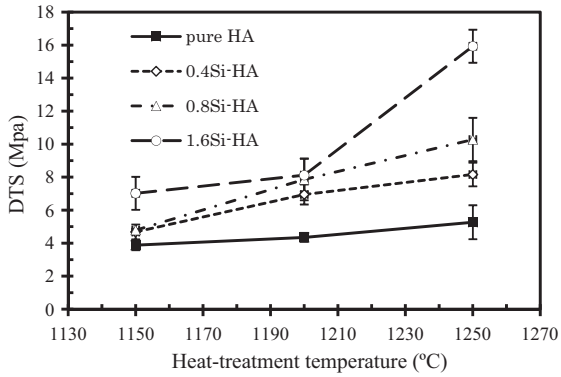

Fig. 8. DTS of HA and Si-HA samples heat-treated at different temperatures of 1150, 1200 and 1250 °C.

samples is less significant and the density of Si-HA samples is close to that of HA sample.

The mechanical strengths of HA and Si-HA were also investigated, namely, the diametral tensile strength (DTS). The relationship between DTS and the heat-treatment temperature is shown in Fig. 8. The DTS of pure HA and 0.4Si-HA samples slightly increases with increasing heat-treatment temperature due to the weak effect of Si on grain growth. In contrast, DTS of 0.8 and 1.6Si-HA samples sharply increases with increasing heat-treatment temperature. The DTS of Si-HA increases with increasing Si contents. It can be explained by the strong effect of Si on the inhibition of grain growth [15]. At 1250 °C, the DTS of 1.6Si-HA is much higher than that of HA and other Si-HAs even though its density is lower. This indicates that the effect of Si on grain size, and consequently on strength, is much more significant than density at high heat-treatment temperatures. The highest DTS value of 15.93 MPa was obtained in 1.6Si-HA sample after heat-treatment at 1250 °C whilst the tensile strength of cencellous bone reported was 10–20 MPa [27]. Thus, the mechanical strength of 1.6Si-HA sample produced in this research work can match the requirement for bone applications.

4. Conclusions

Pure Si-substituted HA with different Si contents of 0.4, 0.8 and 1.6 wt.% was successfully synthesized by the precipitation method. The presence of Si in the HA lattice induced a slight increase in lattice parameters and reduced the grain growth of Si-HA.

The formation of α-TCP phase in 0.8Si-HA sample (clearly at 1250 °C) caused a decrease in density. Si significantly affects the density and diametral tensile strength of Si-HA. The grain size of Si-HA decreases with increasing Si content. The Si content strongly affects the DTS of Si-HA at high temperatures. The DTS increases with increasing heat-treatment temperature and the highest value of 15.93 MPa was obtained in 1.6Si-HA sample after heat-treatment at 1250 °C. The tensile strength of 1.6Si-HA sample are within the requirement for bone application.

Acknowledgements

This research was supported by AUN/SEED-Net and Malaysia Technology Development Corporation (MTDC) Grant No. 6053012. The authors acknowledge Mr. Rashid for obtaining SEM images, Mr. Azam for the FTIR results and Dr. Bui Duc Long for his invaluable suggestions.

References

[1] W.L. Suchanek, P. Shuk, K. Byrappa, R.E. Riman, K.S. TenHuisen, V.F. Janas, Mechanochemical-hydrothermal synthesis of carbonated apatite powders at room temperature, Biomaterials 23 (2002) 699–710.
[2] J.Y. Wong, J.D. Bronzino (Eds.), Biomaterials, CRC Press, Boca Raton, Florida, 2007.
[3] V.R. Maria, A. Daniel, Silicon substituted hydroxyapatite. A method to upgrade calcium phosphate based implants, J. Mater. Chem. 15 (2005) 1509–1516.
[4] F. Balas, J.P. Pariente, M.V. Regi, In vitro bioactivity of silicon-substituted hydroxyapatites, J. Biomed. Mater. Res. 66A (2003) 364–375.
[5] A. Aminian, M. Hashjin, A. Samadikuchaksaraei, F. Bakhshi, F. Gorjipour, A. Farzadi, F. Moztarzadeh, M. Schmcker, Synthesis of silicon-substituted hydroxyapatite by a hydrothermal method with two different phosphorous sources, Ceram. Int. 37 (2011) 1219–2122.
[6] A.M. Pietak, J.W. Reid, M.J. Stott, M. Sayer, Silicon substitution in the calcium phosphate bioceramics, Biomaterials 28 (2007) 4023–4032.
[7] S.M. Best, W. Bonfield, I. Gibson, R. Welwyn, Silicon-substituted apatites and process for the preparation thereof, United States Patent No. 6,312,468 B1, 2001.
[8] A.E. Porter, C.M. Botelho, M.A. Lopes, J.D. Santos, S.M. Best, W. Bonfield, Ultrastructural comparison of dissolution and apatite precipitation on hydroxyapatite and silicon-substituted hydroxyapatite in vitro and in vivo, J. Biomed. Mater. Res. 69A (2004) 670–679.
[9] M. Palard, E. Champion, S. Foucaud, Synthesis of silicate hydroxyapatite $Ca_{10}(PO_4)_{6-x}(SiO_4)_x(OH)_{2-x}$, J. Solid State Chem. 181 (2008) 1950–1960.
[10] S. Sprio, A. Tampieri, E. Landi, M. Sandri, S. Martorana, G. Celotti, G. Logroscino, Physico-chemical properties and solubility behavior of multi-substituted hydroxyapatite powders containing silicon, Mater. Sci. Eng. C 28 (2006) 179–187.
[11] A.E. Porter, S.M. Best, W. Bonfield, Ultrastructural comparison of hydroxyapatite and silicon substituted hydroxyapatite for biomedical application, J. Biomed. Mater. Res. 68A (2004) 133–141.
[12] S.R. Kim, J.H. Lee, Y.T. Kim, D.H. Riu, S.J. Jung, Y.J. Lee, S.C. Chung, Y.H. Kim, Synthesis of Si, Mg substituted hydroxyapatites and their sintering behaviors, Biomaterials 23 (2003) 1389–1398.
[13] I.R. Gibson, S.M. Best, W. Bonfield, Effect of silicon substitution on the sintering and microstructure of hydroxyapatite, J. Am. Ceram. Soc. 85 (11) (2002) 2772–2777.
[14] I.R. Gibson, S.M. Best, W. Bonfield, Chemical characterization of silicon-substituted hydroxyapatite, J. Biomed. Mater. Res. 44 (4) (1999) 422–428.
[15] G. Gasqueres, C. Bonhomme, J. Maquet, F. Babonneau, S. Hayakawa, T. Kanaya, A. Osaka, Revisiting silicate substituted hydroxyapatite by solid-state NMR, Magn. Reson. Chem. 46 (2008) 342–346.
[16] X.L. Tang, X.F. Xiao, R.F. Liu, Structural characterization of silicon-substituted hydroxyapatite synthesized by a hydrothermal method, Mater. Lett. 9 (2005) 3841–3846.
[17] A. Bianco, I. Cacciotti, M. Lombardi, L. Montanaro, Si-substituted hydroxyapatite nanopowders: synthesis, thermal stability and sinterability, Mater. Res. Bull. 44 (2009) 345–354.
[18] J.L. Xu, K.A. Khor, Chemical analysis of silica doped hydroxyapatite biomaterials consolidated by a spark plasma sintering method, J. Inorg. Biochem. 101 (2007) 187–195.
[19] T. Tian, D. Jiang, J. Zhang, Q. Lin, Synthesis of Si-substituted hydroxyapatite by wet mechanochemical method, Mater. Sci. Eng. C 28 (2008) 57–63.
[20] M. Bohner, Silicon-substituted calcium phosphates—A critical view, Biomaterials 30 (2009) 6403–6406.

[21] G.F. Kamst, J. Vasseur, C. Bonazzi, J.J. Bimbenet, A new method for the measurement of the tensile strength of rice grains by using diamentral compression test, J. Food Eng. 40 (1999) 227–232.
[22] A. Aydin, A. Basu, The use of brazilian test as a quantitative measure of rock weathering, Rock Mech. Rock Eng. 39 (1) (2006) 77–85.
[23] A.J. Coreno, A.O. Coreno, R.J.J. Cruz, C.C. Rogríguez, Mechanochemical synthesis of nanocrystalline carbonate-substituted hydroxyapatite, Opt. Mater. 27 (2005) 1281–1285.
[24] E. Zhang, C. Zou, G. Yu, Surface microstructure and cell biocompatibility of silicon-substituted hydroxyapatite coating on titanium substrate prepared by a biomimetic process, Mater. Sci. Eng. C 29 (2009) 298–305.
[25] M. Palard, J. Combes, E. Champion, S. Foucaud, A. Rattner, D. Bernache-Assollant, Effect of silicon content on the sintering and biological behavior of $Ca_{10}(PO4)_{6-x}(SiO4)_x(OH)_{2-x}$ ceramics, Acta Biomater. 5 (2009) 1223–1232.
[26] X.W. Li, H.Y. Yasuda, Y. Umakoshi, Bioactive ceramic composites sintered from hydroxyapatite and silica at 1200 °C: preparation, microstructures and in vitro bone-like layer growth, J. Mater. Sci. Mater. Med. 17 (2006) 573–581.
[27] L.L. Hench, J. Wilson, An Introduction to Bioceramics, World Scientific, Singapore, 1993.